Dalton Transactions

ROYAL SOCIETY OF CHEMISTRY

PAPER

View Article Online
View Journal | View Issue

Cite this: *Dalton Trans.*, 2024, **53**, 12338

Phosphate selective binding and sensing by halogen bonding tripodal copper(II) metallo-receptors in aqueous media†

Hena Bagha,[a] Robert Hein,[a] Jason Y. C. Lim,[a] William K. Myers,[a] Mark R. Sambrook[b] and Paul D. Beer*[a]

Received 30th May 2024,
Accepted 27th June 2024

DOI: 10.1039/d4dt01585a

rsc.li/dalton

Combining the potency of non-covalent halogen bonding (XB) with metal ion coordination, the synthesis and characterisation of a series of hydrophilic XB tripodal Cu(II) metallo-receptors, strategically designed for tetrahedral anion guest binding and sensing in aqueous media is described. The reported metallo-hosts contain a tripodal C_3-symmetric tris-iodotriazole XB donor anion recognition motif terminally functionalised with tri(ethylene glycol) and permethylated β-cyclodextrin functionalities to impart aqueous solubility. Optical UV-vis anion binding studies in combination with unprecedented quantitative EPR anion titration investigations reveal the XB Cu(II) metallo-receptors exhibit strong and selective phosphate recognition over a range of other monocharged anionic species in competitive aqueous solution containing 40% water, notably outperforming a hydrogen bonding (HB) Cu(II) metallo-receptor counterpart. Electrochemical studies demonstrate further the capability of the metallo-receptors to sense anions *via* significant cathodic perturbations of the respective Cu(II)/Cu(I) redox couple.

Introduction

The supramolecular recognition of anions in organic and aqueous media, lies key to the development of artificial receptors for their selective detection, sequestration and transport.[1] Such hosts find important applications in a plethora of biological, medical and environmental fields, for example in the development of bioimmunoassays,[2,3] in drug delivery systems[4,5] and in the remediation of contaminated water.[6,7] Overcoming competitive anion hydration is however one of the main challenges in receptor design, with this problem being especially acute for very hydrophilic anions positioned low in the Hofmeister series such as phosphate.[8] Leading effective strategies so far have centred on the use of highly positively charged hosts, in the form of either organic, biologically inspired molecules, which establish multiple strong electrostatic and hydrogen bonding (HB) interactions to bind selectively the target tetrahedral guest *via* topological complementarity,[8,9] or inorganic metallo-complexes, usually transition metal or lanthanide based, in which the 'hard' metal cation serves as a strong anchoring point for the similarly 'hard' target phosphate oxoanionic species.[10,11] The synergetic combination of these two strategies has also been exploited, although to a lesser extent, in the design of mixed metallo-receptors,[12–14] with Anslyn's phosphate-selective C_3-symmetrical HB Cu(II) tripods being particularly elegant representative examples.[15]

Defined as the attractive non-covalent interaction between an electron-deficient halogen atom and a Lewis base, halogen bonding (XB), has come to the fore in recent years as a remarkably powerful addition to the anion binding supramolecular tool-box.[16] Its stringent directionality requirements compared to traditional HB interactions, coupled with greater hydrophobicity and lower solvent and pH dependency have led to XB host systems often outperforming their more prominent HB host analogues in terms of the strength and selectivity of anion binding.[17,18] While these factors have also advantageously facilitated XB-mediated anion recognition in aqueous solvent media,[19] impressively including in pure water,[20–23] only a handful of XB receptors are known to be capable of selectively recognising phosphate, especially in aqueous containing environments.[24–28] Motivated by this paucity, we recently showed a series of tris(iodotriazole)-containing XB Zn(II) tripodal metallo-receptors to be effective at preferentially binding inorganic phosphate over other more basic oxoanions and the halides in a competitive aqueous-acetonitrile mixture containing 10% water.[29]

With the aim of achieving selective phosphate recognition in an aqueous solution with increased water content, and

[a]*Department of Chemistry, University of Oxford, Chemistry Research Laboratory, Mansfield Road, Oxford, OX1 3TA, UK. E-mail: paul.beer@chem.ox.ac.uk; Tel: +44(0)1865 285142*
[b]*CBR Division, Dstl Porton Down, Salisbury, SP4 0JQ, UK. E-mail: MSAMBROOK@mail.dstl.gov.uk; Tel: +44(0)1980 952077*

† Electronic supplementary information (ESI) available. See DOI: https://doi.org/10.1039/d4dt01585a

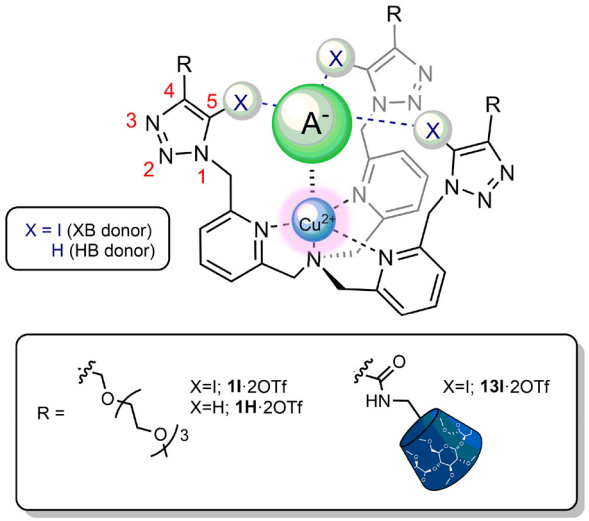

Fig. 1 General design of the 'C_3-symmetric' XB anion recognition motif[29] integrated into hydrophilic functionalised tripodal Cu(II)-receptor frameworks **1I**·2OTf and **13I**·2OTf with the proposed anion binding mode. A^- = anion. (For the full chemical structure of the blue pmβCD 'cone' see Scheme 2.)

anion sensing capability, herein we describe the synthesis of a series of tripodal C_3-symmetrical tris-iodotriazole XB copper(II) metallo-receptor analogues containing hydrophilic polyether and permethylated β-cyclodextrin (pmβCD) functionalities (Fig. 1). Extensive optical UV-vis and unprecedented EPR anion titration investigations reveal the XB metallo-receptors to strongly and selectively bind phosphate over a range of anions in competitive 40% aqueous-containing solvent media. In addition, preliminary electrochemical anion sensing studies demonstrate significant cathodic perturbations of the respective metallo-receptors' Cu(II)/(I) redox couple upon anion binding.

Results and discussion

Synthesis of XB tripodal Cu(II) metallo-receptors

The target XB Cu(II) tripod **1I**·2OTf with hydrophilic solubilising tri(ethylene glycol) (TEG) groups was initially prepared in conjunction with its tris(prototriazole)-containing HB Cu(II) counterpart **1H**·2OTf. The modification of the tripodal termini of **1I**·2OTf with alternative, permethylated β-cyclodextrin (pmβCD) functionalities enabled further systematic investigation into whether changing the solubilising functionalities played any role on the anion recognition capability of receptor **13I**·2OTf.

The first target tris(TEG)-appended XB pyridyl trimer ligand **6I** was synthesised following the multistep synthetic route shown in Scheme 1. TEG-based terminal alkyne **3** was prepared by treating commercially-available TEG monomethyl ether with propargyl bromide under basic conditions using modified literature procedures[30] and subsequently reacted with 6-azidomethyl pyridyl methanol **2**[31] employing Zhu's

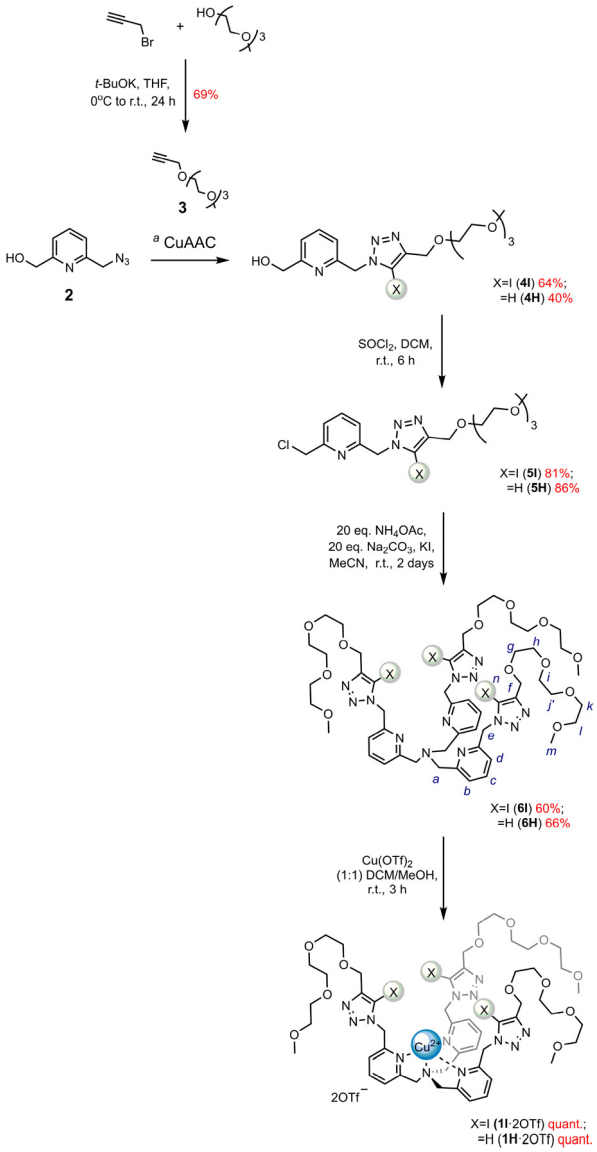

Scheme 1 Synthesis of XB and HB receptors **1I**·2OTf and **1H**·2OTf. [a] For X = I: $Cu(ClO_4)_2{\cdot}6H_2O$, TBTA (cat.), DBU, NaI, MeCN/THF (1 : 1), r.t., 16 h; for X = H: $[Cu(MeCN)_4]PF_6$, DIPEA, DCM, r.t., 48 h.

one-pot 'iodo-click' copper(I)-catalysed azide–alkyne cycloaddition (CuAAC) reaction protocol[32] to afford the XB synthon **4I** in good 64% yield after chromatographic purification. Chlorination with thionyl chloride generated **5I** which was reacted under basic ammonia conditions using an excess of 20 molar equivalents of ammonium acetate, together with an equimolar amount of sodium carbonate to produce the desired XB trimer **6I** in 60% yield. Upon conversion of **5I** to **6I** a pronounced upfield chemical shift change in the ^{1}H NMR spectrum of the crude reaction mixture in $CDCl_3$ was observed for the $H_{a'}$ methylene protons from 4.66 ppm to 3.84 ppm, characteristic of the tertiary *N*-amine region (Fig. S37 ESI†); a single peak at m/z = 1440.2 $[M + H]^+$ in the electrospray ionisation (ESI) mass spectrum of the compound provided further confirmation of tripodal ligand formation (see Fig. S22†).

Complexation of **6I** with a stoichiometric quantity of copper (II) triflate afforded the XB Cu(II)-host **1I**·2OTf. A UV-vis spectroscopy titration experiment revealed the addition of aliquots of the copper salt to an acetonitrile solution of **6I** led to the appearance of a broad peak $\lambda_{abs,max}$ (ε/M^{-1} cm^{-1}) at 640 nm (161) and shoulder peak at 766 nm (98) as well as a visible colour change of the sample solution from colourless to light blue attributed to arise from chelated metal complexation (Fig. 2A).[33] Monitoring the change in absorbance at 640 nm upon addition of increasing equivalents of copper(II) triflate verified the expected 1 : 1 stoichiometry for ligand to metal binding (Fig. 2B). Qualitative analysis of the binding isotherm indicated very strong Cu^{2+} binding affinity, which was too high for quantitative association constant determination in the organic acetonitrile solvent medium. Thus, an Isothermal titration calorimetry (ITC) titration was conducted in unbuffered water, with aliquots of the copper(II) triflate metal salt added to an aqueous solution of **6I** determining an association constant of K_a = 1.55 × 10^6 M^{-1}, as well as the relevant thermodynamic parameters revealing metal complexation to be both enthalpically (ΔH = −29.8 kJ mol^{-1}) and entropically ($-T\Delta S$ = −5.56 kJ mol^{-1}) driven (see the ESI for full ITC details and Fig. S45†).

The counterpart tris(prototriazole)-containing HB Cu(II)-tripod **1H**·2OTf was also prepared *via* analogous procedures (Scheme 1) and both isolated paramagnetic metallo-receptors characterised *via* UV-vis, EPR, HR-MS as well as by electrochemical methods (*vide infra*).

The second XB Cu(II) tripod **13I**·2OTf was prepared *via* adaptation of the synthetic methodology used to construct **1I**·2OTf (Scheme 2). The pmβCD-derived terminal alkyne was first prepared *via* reaction of the activated ester succinimidyl-3-propiolate **7** [34] with amine **8** [19] and a catalytic amount of 4-dimethylaminopyridine (DMAP) overnight to afford **9** in 70% yield after chromatographic purification. An iodo-mediated one-pot CuAAC reaction between **2** and **9** afforded compound **10I**, which was followed by chlorination with thionyl chloride to generate **11I**. Reaction with a large excess of 30 molar equivalents of ammonium acetate and sodium carbonate produced **12I** in 53% yield after purification *via* preparative TLC.‡ A diagnostic, significant upfield shift of the singlet signal (4.64 ppm) of the key $H_{a'}$ methylene protons of monomer **11I**

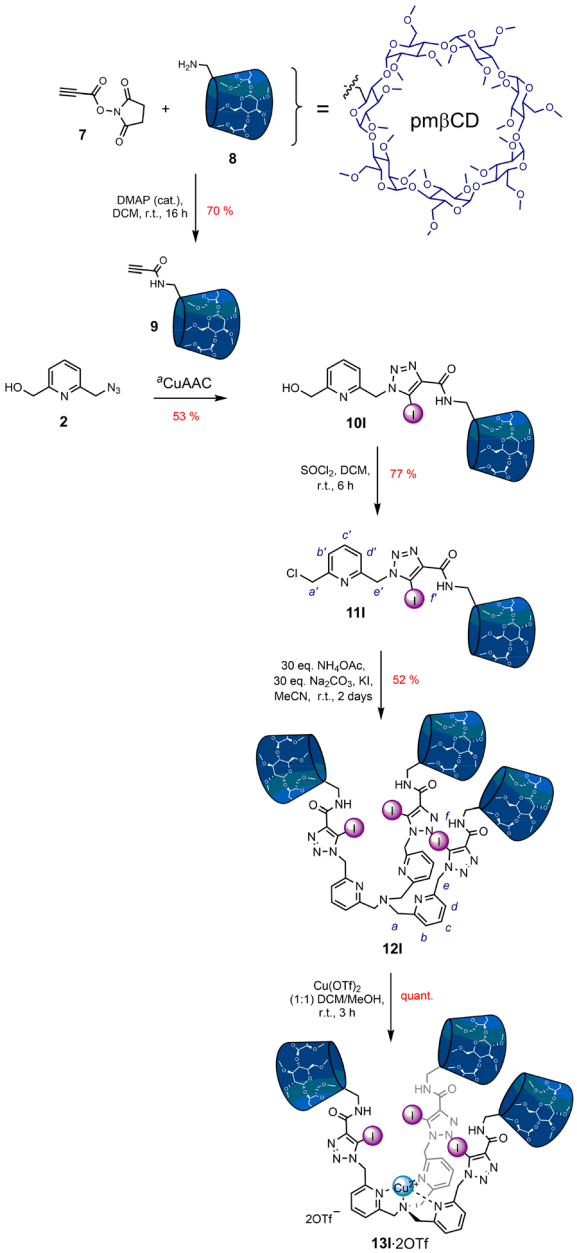

Scheme 2 Synthesis of XB receptor **13I**·2OTf. [a] CuAAC: $Cu(ClO_4)_2{\cdot}6H_2O$, TBTA (cat.), DBU, NaI, MeCN/THF (1 : 1), r.t., 16 h.

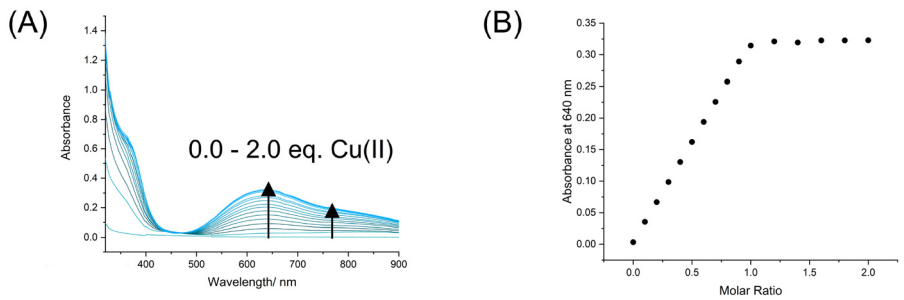

Fig. 2 (A) UV-vis spectra of **6I** upon addition of increments of $Cu(OTf)_2$ up to 2.0 molar equiv. ([host] = 2 mM, CH_3CN, T = 293 K), and (B) the corresponding mole ratio plot.

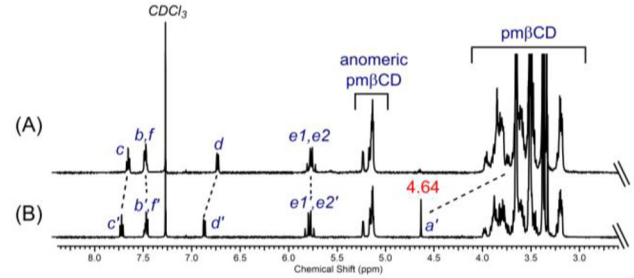

Fig. 3 Stacked ^{1}H NMR spectra of (A) **12I** and (B) synthon **11I** in $CDCl_3$ (500 MHz, T = 298 K). See Scheme 2 for proton assignment. (The methylene H_e protons of both compounds are diastereotopic and hence appear as an AB quartet signal.)

to the main pmβCD region was evidenced in the comparative ^{1}H NMR of trimer **12I** in $CDCl_3$ (see Fig. 3 and S38 ESI†) which along with ESI-MS analysis (m/z = 2627.9 $[M + Na + H]^{2+}$) affirmed the successful transformation to the XB tripodal assembly (Fig. S36†). Complexation of **12I** with copper(II) triflate quantitatively afforded XB Cu(II)-host **13I**·2OTf. Using an analogous ITC titration protocol to **6I**, the Cu(II)-binding properties of **12I** were studied in unbuffered water, determining an association constant of K_a = 1.26 × 10^5 M^{-1} where metal complexation is predominantly enthalpically favoured (ΔH = −28.9 kJ mol^{-1}; $-T\Delta S$ = −0.27 kJ mol^{-1}). **13I**·2OTf was also characterised by UV-vis, EPR and HR-MS methods. The electronic spectrum of **13I**·2OTf in CH_3CN/H_2O 6 : 4 v/v (red dashed line, Fig. 5A) displays a pronounced maximum absorption peak λ_{max} (ε/M^{-1} cm^{-1}) at 645 nm (182) with a much broader shoulder peak at *ca.* 770 nm (119) attributed to arise again from the relevant d–d transitions of the XB ligand chelated to the Cu(II) center.[33]

UV-vis anion binding studies

Quantitative UV-vis titration experiments were performed by adding increasing quantities of anions as their tetrabutylammonium (TBA) salts to separate solutions of **1I**·2OTf and **1H**·2OTf in the CH_3CN/H_2O 6 : 4 v/v solvent mixture (buffered with 10 mM HEPES at pH 6.3). Both receptors exhibited very similar molar extinction coefficients and peak absorption wavelengths $\lambda_{abs,max}$ (ε/M^{-1} cm^{-1}) at 647 nm (117) and 775 nm (91) (shoulder) for **1I**·2OTf and 639 nm (125) and 760 nm (98) (shoulder) for **1H**·2OTf, suggesting that the more electron-deficient, iodotriazole encompassing tripodal ligand framework of **1I**·2OTf did not significantly affect the electronic energy levels of the respective Cu(II) core in mixed aqueous–organic media (Fig. S39 and S41†).

The interactions of Br^-, Cl^-, OAc^- and $H_2PO_4^-$ anions with the Cu(II) center of **1I**·2OTf and **1H**·2OTf led to naked-eye visible colour changes of the host solution from light blue to green, with the presence of an isosbestic point in each of their corresponding UV-vis titration spectra. In each case, a decrease in intensity of the absorption band at *ca.* 640 nm concomitant with an increase in intensity of the broad shoulder peak at *ca.* 770 nm was observed, presumably due to ligand field effects and further implying a similar mode of anion binding within the XB/HB tripodal host interior (Fig. S47†). With the halides, the spectral changes of the latter lower energy band were greater than the former, higher energy band (Fig. 4A) whereas upon addition of oxoanions, both absorption bands exhibited comparable spectral perturbations (Fig. 4B). In contrast, negligible spectral changes were seen during the titrations of NO_3^- indicating that the anion was not interacting appreciably with either receptor.

Global spectral fitting of the UV-vis titration data using the BindFit[35] software monitoring the change in absorbance as a function of anion concentration determined anion association constants summarised in Table 1 (for the corresponding isotherms see Fig. S48 and S49†). All anions were found to bind predominantly *via* a 1 : 2 host : guest stoichiometry with the second binding constant (K_{12}) being of much lower magnitude than the first (K_{11}) suggesting weak peripheral association of the second anion, likely driven by the electrostatic attraction of the host's divalent Cu(II)-metallocentre. Notably, **1I**·2OTf displays strong and selective recognition for $H_2PO_4^-$,§ with an affinity over six times greater than weakest bound Cl^-. Given that the hydration energy of phosphate is the largest of all the anions tested (Table 1), the observed selectivity thus attests to the favourable size and shape match of the TEG-appended XB metallo-tripodal receptor's binding pocket with the target tetrahedral guest (Fig. 4B). In addition **1I**·2OTf exhibited a distinct Hofmeister preference for $Br^- > Cl^-$. Importantly, the HB receptor **1H**·2OTf although also being phosphate selective, displayed attenuated anion binding in all cases, with very modest discrimination between Br^- and Cl^-. The large difference between the magnitudes of the phosphate association constants of the two receptors in particular, with the value calculated for **1I**·2OTf over three-times greater than **1H**·2OTf, provides a very rare demonstration of the superior ability of XB to enhance hard oxoanion recognition in highly competitive 40% aqueous–organic solvent mixtures. Compared to the current cadre of reported XB phosphate receptors,[24–29] **1I**·2OTf therefore constitutes a very potent XB host capable of discriminating phosphate in aqueous media.

The demonstration of selective inorganic monophosphate binding by both XB **1I**·2OTf and HB **1H**·2OTf receptors prompted us to also investigate their ability to bind a simple phosphate-ester and a higher-order polyphosphate species, specifically pinacolyl methyl phosphonate (PMP), the innocuous hydrolysis product of the 'G-series' chemical warfare nerve agent soman (GD)[38] and inorganic pyrophosphate (PPi),

‡The usual 20 equivalents of NH_4OAc utilised in previous tripodal ligand formation procedures (see Scheme 1) was increased to 30 equivalents given the propensity of reagents to form inclusion complexes with the β-cyclodextrin 'cone'.

§It should be noted that at the working pH 6.3 maintained in the UV-vis experiments, inorganic phosphate exists about 88% as $H_2PO_4^-$ and 12% as HPO_4^{2-} (calculated using the HyperQuad[37] software), hence here we have referred to the former dominant diprotic form as representative of the total monophosphate species.

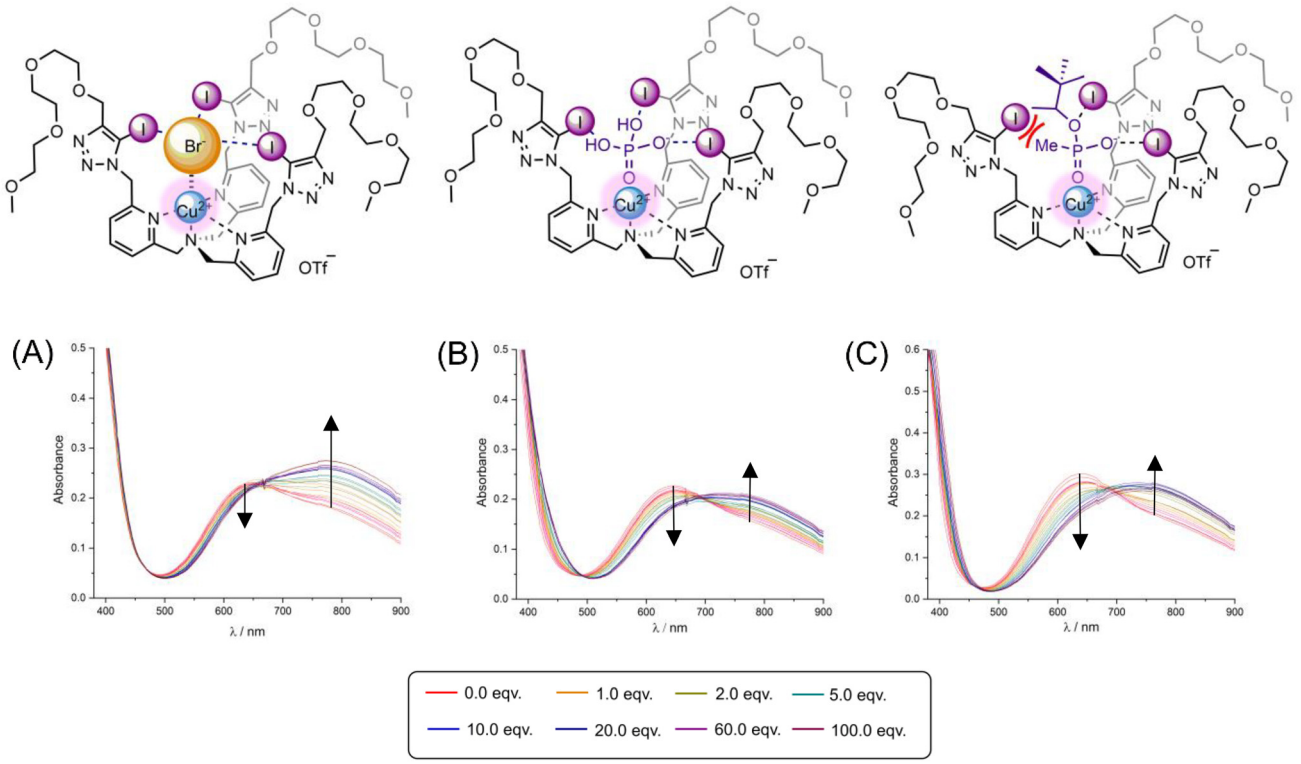

Fig. 4 UV-vis anion titration spectra of **1I**·2OTf in the presence of up to 100 equivalents of (A) TBA Br, (B) TBA H_2PO_4 and (C) TBA PMP ([host] = 2 mM, CH_3CN/H_2O 6 : 4 buffered with 10 mM HEPES at pH 6.3, T = 293 K).

Table 1 Anion association constants (K_a/M^{-1}) of **1I**·2OTf and **1H**·2OTf[a]

Anion	ΔG_{hyd} [b] (kJ mol^{--1})	**1I**·2OTf	**1H**·2OTf
Cl^-	−340	K_{11} = 379 (15) K_{12} = 16	121 (3)
Br^-	−315	K_{11} = 834 (38) K_{12} = 23	K_{11} = 108 (2) K_{12} = 7
I^-	−275	—[c]	—[c]
NO_3^-	−300	NB[d]	NB[d]
OAc^-	−365	K_{11} = 435 (20) K_{12} = 21	—[e]
$H_2PO_4^-$	−465	K_{11} = 2816 (309) K_{12} = 3	K_{11} = 745 (25) K_{12} = 1
PMP^-	n/a	K_{11} = 1094 (68) K_{12} = 73	K_{11} = 772 (63) K_{12} = 11

[a] A 1 : 2 host–guest binding model, unless otherwise stated, was used to determine K_a values from global fitting of the UV-vis titration spectra, monitoring the change in absorption from 800–850 nm, using BindFit;[35] anions added as their TBA salts; ([host] = 2 mM, CH_3CN/H_2O 6 : 4, T = 293 K); errors (±) in parenthesis (<11%). [b] Values reported by Marcus.[36] [c] Titration not performed as I^- is easily oxidised in the presence of Cu(II). [d] NB: no binding. Spectral changes too little to accurately determine association constants. [e] Multiple complex binding equilibria. Unable to fit data to 1 : 1, 1 : 2 or 2 : 1 host–guest models.

respectively. Upon the addition of TBA PMP, pronounced optical perturbations analogous to those elicited with $H_2PO_4^-$ were evidenced in the individual absorption spectra of **1I**·2OTf (Fig. 4C) and **1H**·2OTf (Fig. S47†) and the organophosphonate found to associate with the host similarly with a 1 : 2 host–guest stoichiometry (Table 1). Yet again, the XB receptor proved to be the stronger complexant, binding PMP^- with a larger affinity than the protic counterpart thus highlighting the applicability of XB as a potent supramolecular interaction to further exploit for the enhanced recognition of its parent GD compound as well as other, more toxic 'G-series' substances.[39] The lower association constant value of PMP^- with **1I**·2OTf compared to $H_2PO_4^-$ is unsurprising given the steric demands of the much larger aliphatic group functionalised phosphonate, resulting in a less complementary fit within the XB host's tetrahedral cavity: possibly, the alkyl substituent protons of the organophosphonate's phosphate 'head' might impose a steric clash with one of the voluminous iodine atoms of a convergent iodotriazole binding unit (red lines, Fig. 4C).

In contrast, the addition of aliquots of TBA_3 PPi to **1I**·2OTf elicited explicitly larger spectral changes with a dramatic intensity decrease in *both* of the absorption bands of the XB Cu(II)-host (Fig. S47†). Compared to the other anions tested, only unidirectional changes were observed with PPi^{3-} suggesting that it was being bound *via* a different coordination stoichiometry perhaps simultaneously 'bridging' the metal centers of two individual XB hosts, in a similar manner as when coordinating to the structurally related bimetallic Zn(II)–dipicolylamine compounds and/or di-nuclear Cu(II) tripodal amine complexes.[40–42] Attempts to fit the titration data to various binding models of 2 : 1 as well as 1 : 1 and 1 : 2 host–guest stoichiometries unfortunately failed to determine quantitative association constant data.

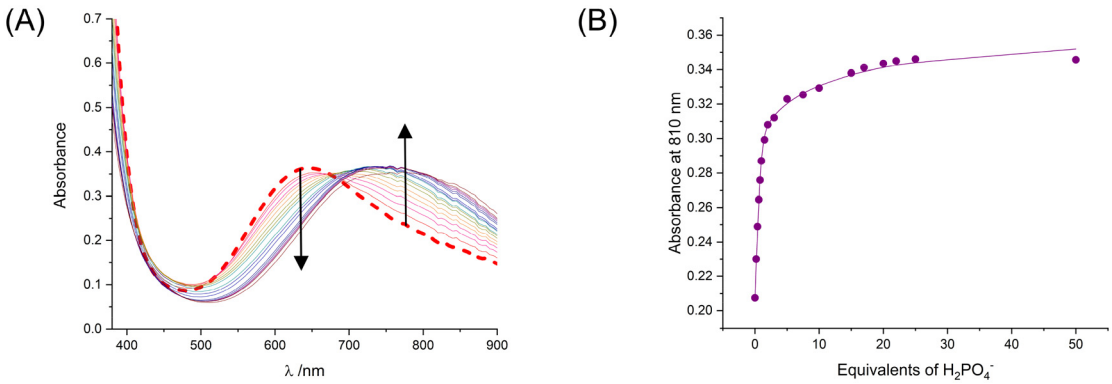

Fig. 5 (A) UV-vis titration spectra of **13I**·2OTf (red dashed line) with up to 100 equivalents of TBA H_2PO_4 ([host] = 2 mM, CH_3CN/H_2O 6 : 4 buffered with 10 mM HEPES at pH 6.3, T = 293 K), (B) the corresponding isotherm monitoring the change in absorbance from 800–850 nm *vs.* equivalents of anion.

Similar spectral perturbations of the host's d–d bands were observed upon the addition of aliquots of TBA H_2PO_4 to **13I**·2OTf as **1I**·2OTf, with the progressive decrease in intensity of the initial higher energy absorption band (at 645 nm) and comparable increase in intensity of the initial lower energy shoulder peak (at *ca.* 770 nm) suggestive of a similar mode of anion binding within the tripodal XB cavity (Fig. 5A). Global spectral fitting of the UV-vis titration data using the BindFit[35] software notably revealed an enhancement in the binding of $H_2PO_4^-$ with **13I**·2OTf (Fig. 5B), with the determined 1 : 2 stoichiometric association constants of K_{11} = 9442 ± 944 M^{-1} and K_{12} = 40 ± 2 M^{-1} being *ca.* thrice as large in magnitude compared to **1I**·2OTf (*cf.* Table 1). The observed increased phosphate anion affinity may arise from the donor ability of the XB iodotriazoles being augmented *via* intramolecular N–H···I HB interactions from the neighbouring amide functionalities of the host's pmβCD-derived 'arms' which promote the synergistic binding of the target tetrahedral guest *via* multiple 'hydrogen bonding-enhanced halogen bonding' (HBeXB) interactions (Fig. 6).[43,44]

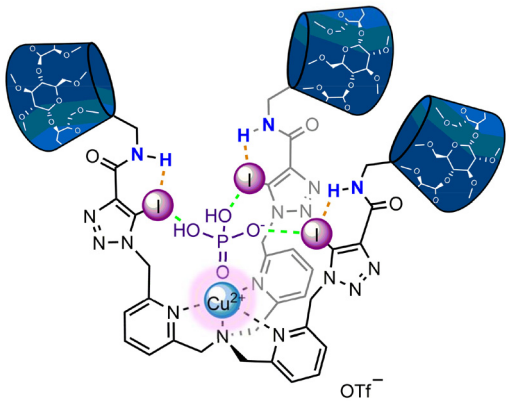

Fig. 6 The envisioned binding mode of XB receptor **13I**·2OTf with $H_2PO_4^-$ (intramolecular N–H···I HB indicated by orange dashed lines; N–H HBeXB interactions indicated by green dashed lines).

EPR anion binding studies with 1I/H·2OTf

To complement the UV-vis anion titration experiments, the host–guest properties of **1I/H**·2OTf towards Br^- and $H_2PO_4^-$ were also investigated *via* EPR spectroscopy. The X-band continuous wave (CW) EPR spectra of both 'free' receptors **1I**·2OTf and **1H**·2OTf were first recorded in the frozen buffered CH_3CN/H_2O 6 : 4 v/v solvent mixture at 85 K (see Fig. 7A and B, bold red lines and Fig. S39 and S41, ESI†). The XB host displayed an axial signature characterised by the principal g values of $g_{\|}$ = 2.225 and $g_{\perp}$ = 2.056 ($A_{\|}$ = 183.0 × 10^{-4} cm^{-1}) with the classic four-line splitting pattern in the parallel region arising from the hyperfine interactions between the unpaired Cu(II) electron and the two principle ^{63}Cu and ^{65}Cu paramagnetic nuclei.¶ Notably, these $g_{\|} > g_{\perp}$ values are quite unusual for tris-(2-pyridylmethyl)amine (TPMA) based Cu(II)-complexes which typically present $g_{\perp} > g_{\|}$ values that denote a 5-coordinate Cu(II) environment, where the metal cation is ligated by four nitrogen atoms of the tetradentate TPMA subunit and also one solvent molecule (either CH_3CN or H_2O), predominantly in a trigonal bipyramidal (TBP) geometry.[45–47] The obtained $A_{\|}$ value is also much larger than the ones classically encountered for TBP Cu(II)-centers ($A_{\|}$ < 80 × 10^{-4} cm^{-1}).[48] With these observations in mind and having previously evidenced the additional N^2-coordination of two of the iodotriazoles to the Zn(II) center in the X-ray crystallographic solid state structure of the tris(ferrocene) receptor analogue,[29] a similar 6-coordinate Cu(II) centre of **1I**·2OTf in *frozen* solution thus seems likely.‖ Due to the lack of spectroscopic characterisation

¶($2NI$ + 1 = 4, where N is the number of nuclei felt by the unpaired electron and I is the nuclear spin quantum number, which for a Cu(II) nucleus is I = 3/2).

‖The very fast relaxation times of the two *dynamic* $T1$ (spin–lattice) and $T2$ (spin–spin) relaxation processes often observed at room temperature (*e.g.* for transition-metal complexes) and crucial in the EPR experiment, inevitably lead to extensive broadening of the acquired spectrum such that effectively no EPR signal is observed (half linewidth = $1/T2 + 1/2T1$, as also dictated by Heisenberg's uncertainty principle).[49] Consequently, EPR measurements are routinely undertaken at cryogenic temperatures (*i.e.* in frozen solution) to increase the $T1$ and $T2$ times of such 'fast relaxing systems' thus leading to better-resolved EPR spectra.

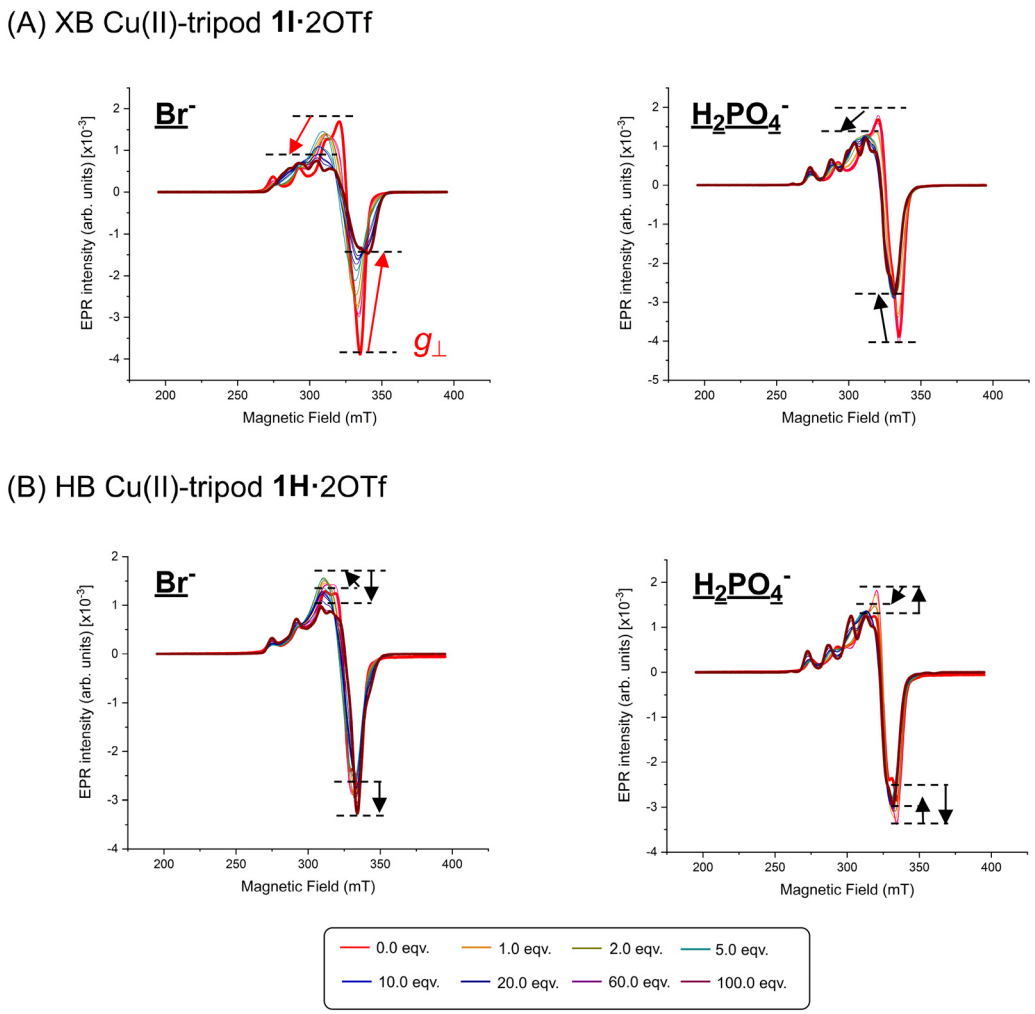

Fig. 7 CW EPR titration spectra of receptors (A) **1I**·2OTf and (B) **1H**·2OTf in the presence of increasing quantities of anions ([host] = 2 mM, CH_3CN/H_2O 6 : 4 buffered with 10 mM HEPES at pH 6.3, T = 85 K). EPR signature changes specifically in the perpendicular region of the titration spectra are indicated by the arrows.

of such '4 + 2' coordinated Cu(II)–TPMA complexes in the literature however, the unambiguous assignment of an octahedral coordination geometry is rather complicated. Receptor **1H**·2OTf exhibited virtually identical EPR parameters of $g_{\|}$ = 2.285 and $g_{\perp}$ = 2.055 apart from a very small difference of the $A_{\|}$ value ($A_{\|}$ = 180.0 × 10^{-4} cm^{-1}) suggesting, similarly to the UV-vis characterisation data, little influence of the iodotriazoles on the hyperfine coupling and hence degree of delocalisation of the unpaired d-electron from the respective paramagnetic Cu(II) center.

EPR anion titration investigations were performed by adding increasing aliquots of anions (up to 100 equivalents) as their TBA salts to separate solutions of the XB and HB Cu(II)-tripodal receptors and the CW EPR spectra recorded at 85 K (full experimental details of the EPR titration protocol are included in the ESI†). Characteristic changes in the EPR spectral signatures and intensities of **1I**·2OTf and **1H**·2OTf were afforded upon addition of the Br^- and $H_2PO_4^-$ guests (Fig. 7). Firstly, in all cases, the original quadruple line-splitting pattern contained multiple overlapping contributions in both parallel and perpendicular regions (*i.e.* >four-line splitting) thus indicative of a 'mixed' equilibrium species (presumably the 'free' host and 'bound' host–guest adduct) present in frozen aqueous–organic solution. A pronounced overall reduction in intensity of the $g_{\perp}$ contribution of both **1I**·2OTf and **1H**·2OTf with both anions was further qualitatively observed upon signal saturation – this is particularly evident in the perpendicular region of the XB receptor with Br^- (Fig. 7A, red arrows). Indeed whilst these qualitative differences show that it is possible to detect anion binding through form of a simple ligand-exchange at the metal center using EPR spectroscopy, the complex signatures of the titration spectra require further extensive simulation work (beyond the scope of this study) to separate the overlapping contributions and hence extract the corresponding g values and hyperfine EPR parameters giving insight to the *exact* nature of the anion interaction and axial Cu(II) coordination site.

For this reason, a global spectral fitting strategy of the EPR titration data was adopted, monitoring the changes in EPR

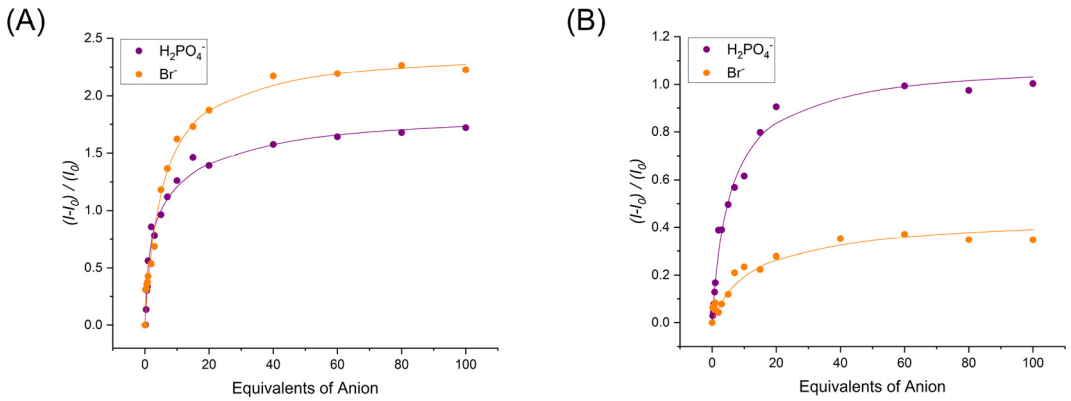

Fig. 8 EPR anion titration isotherms of receptor (A) **1I**·2OTf and (B) **1H**·2OTf, monitoring the change in signal intensity from 280–290 mT *vs.* equivalents of anion added ([host] = 2 mM, CH_3CN/H_2O 6 : 4 buffered with 10 mM HEPES at pH 6.3, T = 85 K).

intensity (within the limits of the $A_{\|}$ and $g_{\|}$ extrema) as a function of anion concentration (Fig. 8) which allowed for the determination of association constants of 1 : 2 stoichiometry using the BindFit[35] software as summarised in Table 2. Pleasingly, these EPR titration binding constants are in alignment with the results obtained from the corresponding UV-vis anion titrations: the XB receptor once more, not only exhibited preferential binding of $H_2PO_4^-$ over Br^- but importantly also superior binding of anions than the HB counterpart in both cases (*cf.* Table 1). To the best of our knowledge, *quantitative* anion titrations with small artificial receptors such as these *via* EPR spectroscopy remain unprecedented in the literature – only calixarene-based azacryptand Cu(II) funnel complexes have been reported by Reinaud and co-workers for the quantitative EPR detection of *neutral* alcohol, amine and nitrile guests.[45–47] This experimental data thus serves to highlight the applicability of EPR as a detection tool for the sensing of anionic guests as well as the determination of their association constants.

Table 2 Anion association constants (K_a/M^{-1}) of **1I**·2OTf and **1H**·2OTf from EPR titrations[a]

Anion	**1I**·2OTf	**1H**·2OTf
Br^-	K_{11} = 369 (22)	K_{11} = 101 (7)
	K_{12} = 55	K_{12} = 16
$H_2PO_4^-$	K_{11} = 1641 (102)	K_{11} = 743 (65)
	K_{12} = 36	K_{12} = 59

[a] A 1 : 2 host–guest binding model unless otherwise stated, was used to determine K_a values from global fitting of the EPR titration spectra, monitoring the change in signature intensity from 280–290 mT, using BindFit;[35] anions added as their TBA salts; ([host] = 2 mM, CH_3CN/H_2O 6 : 4, T = 85 K); errors (±) in parenthesis (<11%).

Preliminary electrochemical anion sensing studies with 1I/H·2OTf

The success of **1I/H**·2OTf as effective optical sensors and EPR probes for $H_2PO_4^-$ encouraged us to explore the possibility of exploiting the hosts' cupric metal centre further for electrochemical phosphate sensing *via* the Cu^{II}/Cu^{I} redox couple. The redox properties of **1I**·2OTf and **1H**·2OTf were initially investigated *via* cyclic voltammetry (CV) in anhydrous CH_3CN (0.1 M $TBAClO_4$ supporting electrolyte solution) and pure water (0.05 M KPF_6 supporting electrolyte solution) solvents as well as in various intermediate CH_3CN/H_2O mixtures, using a Ag/AgCl reference electrode (see ESI† for full reversibility details). Both receptors were found to display explicit solvent dependent redox behaviour.

In anhydrous CH_3CN, both **1I**·2OTf and **1H**·2OTf were electrochemically-active and displayed a well-defined, single quasi-reversible one-electron wave attributed to the Cu^{II}/Cu^{I} redox couple, with the more anodic $E_{1/2}$ value of +74 mV of the XB host *versus* −179 mV of the HB counterpart (both *vs.* Fc/Fc^+) consistent with the increased electron-withdrawing nature of the iodotriazoles disfavouring oxidation of the Cu center (Fig. S50 and S52†). The marked 253 mV difference between the two $E_{1/2}$ values is particularly noteworthy and as previously suggested by the EPR characterisation data, indicates the N^2-coordination of the XB/HB-triazoles to the metal core, which are thus able to *directly* exert their electronic influences on the redox properties of the Cu center in organic media. Contrastingly, whilst the XB and HB Cu(II)-receptors retained redox quasi-reversibility in various CH_3CN/H_2O solvent mixtures, a significantly distorted anodic peak was observed in each case particularly at higher scan rates. This was exacerbated in pure water (see Fig. S54 and S56†) and postulated to arise from the 'static' N^2-ligation of the XB/HB-triazoles to the Cu center, as strongly suggested by the earlier investigative EPR data. Indeed, the more anodic $E_{1/2}$ values of +174 mV of the XB host and +89 mV of the HB counterpart (both *vs.* Ag/AgCl) in pure water compared to those in CH_3CN (where the triazole coordination is 'dynamic') lend credence to this hypothesis. Additionally, the much smaller 85 mV discrepancy between these $E_{1/2}$ values likely results from the better stabilisation of the dicationic *vs.* monocationic Cu state due to the increased polarity of the all-aqueous solvent medium.

Owing to the complex voltammetric behaviour exhibited by **1I/H**·2OTf in aqueous containing media, their redox anion

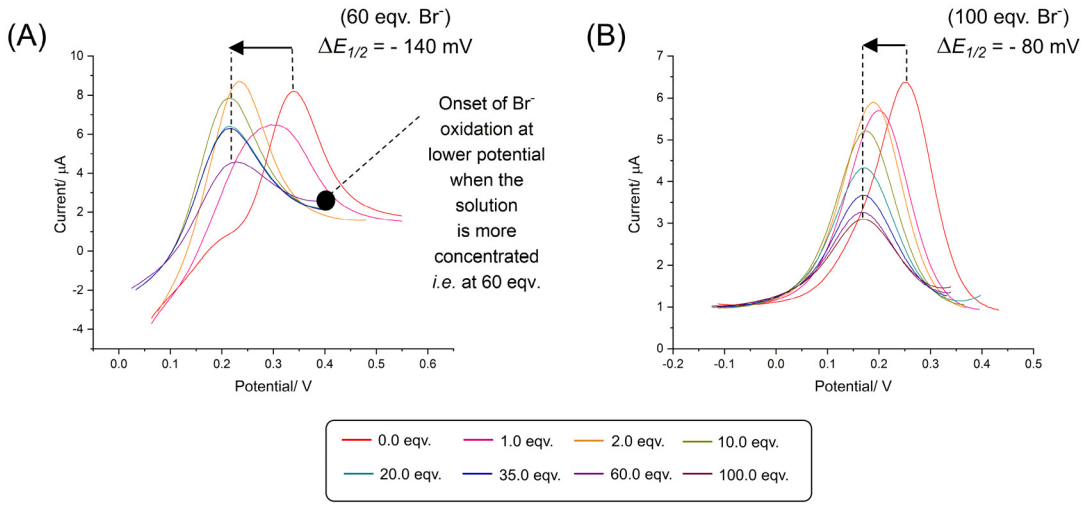

Fig. 9 Square wave voltammograms of receptors (A) **1I**·2OTf and (B) **1H**·2OTf with incremental quantities of TBA Br ([host] = 0.5 mM, electrolyte: 0.1 M $TBAClO_4$ in anhydrous CH_3CN, T = 293 K). All potentials taken in reference to the Ag/AgCl reference electrode (leak free). (The distorted red baseline in (A) arises from the need of having to adjust the potential range during the titration to prevent Br^- oxidation.)

sensing properties were probed only in anhydrous CH_3CN (containing 0.1 M $TBAClO_4$ as supporting electrolyte) using square-wave voltammetry (SWV). Due to precipitation problems with phosphate, preliminary electrochemical anion titrations were restricted to bromide. The addition of excess TBA Br (up to 100 equivalents) induced significant cathodic perturbations of the respective Cu^{II}/Cu^{I} redox couples of both XB and HB receptors arising from halide anion binding stabilising the Cu(II) oxidation state (Fig. 9). In both cases, a swift plateauing of the voltammetric response was observed further indicative of strong binding (Fig. 10). Notably however, the XB host exhibited a much larger magnitude of cathodic shift (−140 ± 5 mV) at saturation compared to the protic analogue (−80 ± 5 mV) clearly highlighting the dominant role played by the XB donor groups for redox anion sensing. The very large magnitudes of these cathodic shifts further enabled the quantitative analysis of the respective titration isotherms according to the established 1 : 1 host–guest stoichiometric Nernst model (eqn (1)):[50]

$$\Delta E = -\frac{RT}{nF}\ln\frac{(1 + K_{ox}[A^-])}{(1 + K_{red}[A^-])} \quad (1)$$

which revealed that the anion association constant of the oxidised metallo-receptor (K_{ox}) with the halide was, as expected, larger than the reduced form ($K_{ox} > K_{red}$) and that indeed, the XB receptor demonstrated a magnified switching on of Br^- binding (K_{ox}/K_{red} = 65 074/289 M^{-1}) compared to the HB analogue (K_{ox}/K_{red} = 15 734/581 M^{-1}). In particular, these amplified halide anion-induced voltammetric responses of **1I**·2OTf and **1H**·2OTf compared to those observed with their electrochemically active tris(ferrocene) Zn(II)-receptor counterparts[29] convey not only the efficacy of the Cu^{II}/Cu^{I} redox couple as an electrochemical transduction entity but also the potency of utilising the host's metal epitope as a *direct probe* for the anion binding event (Fig. 4A) – which for self-evident reasons, exhibits a greater sensitivity to the recognition process as opposed to the *through-bond* communicative pathways between the anion binding cavity and redox reporter group.[29]

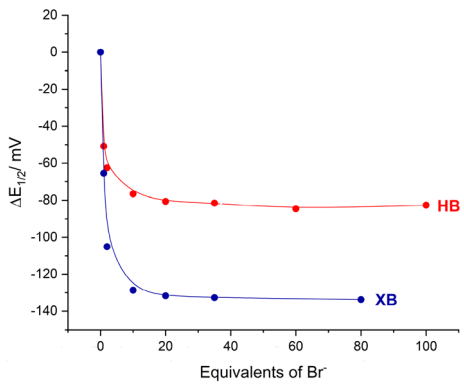

Fig. 10 Electrochemical anion titration isotherms. Shift of the half-wave potential ($\Delta E_{1/2}$) of the Cu^{II}/Cu^{I} redox couple of **1I**·2OTf (blue) and **1H**·2OTf (red) in the presence of Br^-.

Conclusions

In conclusion, a series of strategically designed, hydrophilic XB tripodal Cu(II) metallo-receptors **1I**·2OTf and **13I**·2OTf were synthesised and demonstrated to be effective at selectively recognising and sensing inorganic monophosphate over a range of other monoanionic species in aqueous media containing 40% water. Extensive UV-vis spectrophotometric anion titration studies, notably accompanied by a naked-eye colour change response, revealed that **1I**·2OTf bound $H_2PO_4^-$ strongly (K_a = 2816 M^{-1}) with an affinity over six times greater than the

weakest bound Cl^-, which was attributed to the complementary size and shape match between the tetrahedral anion and the XB tripodal cavity. Importantly, the phosphate association constant value for **1I**·2OTf was notably of a significantly larger magnitude than that obtained with the HB receptor counterpart **1H**·2OTf further championing and advancing XB as a more effective interaction than HB for hard oxoanion binding in aqueous environments. Similarly augmented binding of the monophosphate-ester PMP^- was evidenced with **1I**·2OTf compared to **1H**·2OTf thus also highlighting the applicability of XB as a worthwhile supramolecular interaction to potentially exploit for the enhanced recognition of toxic 'G-series' substances as well as their innocuous hydrolysis products. Furthermore, an impressive *ca.* three-fold enhancement in phosphate binding affinity was achieved with **13I**·2OTf compared to **1I**·2OTf, with the presence of the host's XB donor iodotriazole *and* conjugated HB donor NH amide functionalities bringing to light the synergistic interplay of these two, often competing, interactions in the binding process.

Importantly both XB/HB Cu(II) receptors **1I/H**·2OTf were also demonstrated to be highly sensitive EPR anion sensing probes, wherein the determination of quantitative anion binding constant data was achieved for the first time. The Cu(II) metallo-receptors also proved to be effective electrochemical anion sensors capable of sensing Br^- *via* cathodic shift perturbations of their respective Cu^{II}/Cu^{I} redox couples. Further exploitation of the 'C_3-symmetric' XB motif[29] for XB-mediated oxoanion recognition and sensing applications in aqueous media is continuing in our laboratories.

Data availability

The data supporting this article have been included as part of the ESI.†

Conflicts of interest

There are no conflicts to declare.

Acknowledgements

H. B. thanks Dstl for a DTA studentship.

References

1 L. K. Macreadie, A. M. Gilchrist, D. A. McNaughton, W. G. Ryder, M. Fares and P. A. Gale, *Chem*, 2022, **8**, 46–118.
2 S. Faulkner, S. J. A. Pope and B. P. Burton-Pye, *Appl. Spectrosc. Rev.*, 2005, **40**, 1–31.
3 S. E. Bodman and S. J. Butler, *Chem. Sci.*, 2021, **12**, 2716–2734.
4 X. Ma and Y. Zhao, *Chem. Rev.*, 2015, **115**, 7794–7839.
5 H. Cui and B. Xu, *Chem. Soc. Rev.*, 2017, **46**, 6430–6432.
6 B. O. Okesola and D. K. Smith, *Chem. Soc. Rev.*, 2016, **45**, 4226–4251.
7 H. Wang, X. Ji, M. Ahmed, F. Huang and J. L. Sessler, *J. Mater. Chem. A*, 2019, **7**, 1394–1403.
8 A. E. Hargrove, S. Nieto, T. Zhang, J. L. Sessler and E. V. Anslyn, *Chem. Rev.*, 2011, **111**, 6603–6782.
9 S. Pal, T. K. Ghosh, R. Ghosh, S. Mondal and P. Ghosh, *Coord. Chem. Rev.*, 2020, **405**, 213128.
10 K. A. Jolliffe, *Acc. Chem. Res.*, 2017, **50**, 2254–2263.
11 M. V. R. Raju, S. M. Harris and V. C. Pierre, *Chem. Soc. Rev.*, 2020, **49**, 1090–1108.
12 O. Francesconi, M. Gentili, F. Bartoli, A. Bencini, L. Conti, C. Giorgi and S. Roelens, *Org. Biomol. Chem.*, 2015, **13**, 1860–1868.
13 S. J. Butler, *Chem. – Eur. J.*, 2014, **20**, 15768–15774.
14 R. Mailhot, T. Traviss-Pollard, R. Pal and S. J. Butler, *Chem. – Eur. J.*, 2018, **24**, 10745–10755.
15 S. L. Tobey, B. D. Jones and E. V. Anslyn, *J. Am. Chem. Soc.*, 2003, **125**, 4026–4027.
16 L. C. Gilday, S. W. Robinson, T. A. Barendt, M. J. Langton, B. R. Mullaney and P. D. Beer, *Chem. Rev.*, 2015, **115**, 7118–7195.
17 J. Y. C. Lim and P. D. Beer, *Chem*, 2018, **4**, 731–783.
18 R. Hein and P. D. Beer, *Chem. Sci.*, 2022, **13**, 7098–7125.
19 T. Bunchuay, A. Docker, A. J. Martinez-Martinez and P. D. Beer, *Angew. Chem., Int. Ed.*, 2019, **58**, 13823–13827.
20 M. J. Langton, S. W. Robinson, I. Marques, V. Félix and P. D. Beer, *Nat. Chem.*, 2014, **6**, 1039–1043.
21 S. P. Cornes, M. R. Sambrook and P. D. Beer, *Chem. Commun.*, 2017, **53**, 3866–3869.
22 A. Borissov, I. Marques, J. Y. C. Lim, V. Félix, M. D. Smith and P. D. Beer, *J. Am. Chem. Soc.*, 2019, **141**, 4119–4129.
23 E. J. Mitchell, A. J. Beecroft, J. Martin, S. Thompson, I. Marques, V. Félix and P. D. Beer, *Angew. Chem., Int. Ed.*, 2021, **60**, 24048–24053.
24 M. Cametti, K. Raatikainen, P. Metrangolo, T. Pilati, G. Terraneo and G. Resnati, *Org. Biomol. Chem.*, 2012, **10**, 1329–1333.
25 B. Chowdhury, S. Sinha and P. Ghosh, *Chem. – Eur. J.*, 2016, **22**, 18051–18059.
26 F. Zapata, A. Caballero and P. Molina, *Eur. J. Inorg. Chem.*, 2017, **2017**, 237–241.
27 F. Zapata, L. González, A. Caballero, A. Bastida, D. Bautista and P. Molina, *J. Am. Chem. Soc.*, 2018, **140**, 2041–2045.
28 J. Y. C. Lim and P. D. Beer, *New J. Chem.*, 2018, **42**, 10472–10475.
29 H. Bagha, R. Hein, J. Y. C. Lim, C. B. Durr, M. R. Sambrook and P. D. Beer, *Chem. – Eur. J.*, 2024, **30**, e202302775.
30 T. Shiraki, A. Dawn, Y. Tsuchiya and S. Shinkai, *J. Am. Chem. Soc.*, 2010, **132**, 13928–13935.
31 T. Zhang and E. V. Anslyn, *Tetrahedron*, 2004, **60**, 11117–11124.
32 W. S. Brotherton, R. J. Clark and L. Zhu, *J. Org. Chem.*, 2012, **77**, 6443–6455.

33 P. J. Arnold, S. C. Davies, J. R. Dilworth, M. C. Durrant, D. V. Griffiths, D. L. Hughes, R. L. Richards and P. C. Sharpe, *J. Chem. Soc., Dalton Trans.*, 2001, 736–746.
34 J. Chao, W.-Y. Huang, J. Wang, S.-J. Xiao, Y.-C. Tang and J.-N. Liu, *Biomacromolecules*, 2009, **10**, 877–883.
35 P. Thordarson, *Chem. Soc. Rev.*, 2011, **40**, 1305–1323.
36 Y. Marcus, *J. Chem. Soc., Faraday Trans.*, 1991, **87**, 2995–2999.
37 L. Alderighi, P. Gans, A. Ienco, D. Peters, A. Sabatini and A. Vacca, *Coord. Chem. Rev.*, 1999, **184**, 311–318.
38 K. Kim, O. G. Tsay, D. A. Atwood and D. G. Churchill, *Chem. Rev.*, 2011, **111**, 5345–5403.
39 M. R. Sambrook and S. Notman, *Chem. Soc. Rev.*, 2013, **42**, 9251–9267.
40 D. H. Lee, S. Y. Kim and J.-I. Hong, *Angew. Chem., Int. Ed.*, 2004, **43**, 4777–4780.
41 S. J. Butler and K. A. Jolliffe, *Chem. – Asian J.*, 2012, **7**, 2621–2628.
42 S. Watchasit, A. Kaowliew, C. Suksai, T. Tuntulani, W. Ngeontae and C. Pakawatchai, *Tetrahedron Lett.*, 2010, **51**, 3398–3402.
43 A. M. S. Riel, R. K. Rowe, E. N. Ho, A.-C. C. Carlsson, A. K. Rappé, O. B. Berryman and P. S. Ho, *Acc. Chem. Res.*, 2019, **52**, 2870–2880.
44 R. P. Orenha, S. S. P. Furtado, G. F. Caramori, M. J. Piotrowski, A. Muñoz-Castro and R. L. T. Parreira, *New J. Chem.*, 2023, **47**, 4439–4447.
45 N. Le Poul, B. Douziech, J. Zeitouny, G. Thiabaud, H. Colas, F. Conan, N. Cosquer, I. Jabin, C. Lagrost, P. Hapiot, O. Reinaud and Y. Le Mest, *J. Am. Chem. Soc.*, 2009, **131**, 17800–17807.
46 G. Izzet, X. Zeng, H. Akdas, J. Marrot and O. Reinaud, *Chem. Commun.*, 2007, 810–812.
47 G. Thiabaud, A. Brugnara, M. Carboni, N. Le Poul, B. Colasson, Y. Le Mest and O. Reinaud, *Org. Lett.*, 2012, **14**, 2500–2503.
48 D. K. Chand and P. K. Bharadwaj, *Inorg. Chem.*, 1996, **35**, 3380–3387.
49 M. M. Roessler and E. Salvadori, *Chem. Soc. Rev.*, 2018, **47**, 2534–2553.
50 R. Oliveira, S. Groni, C. Fave, M. Branca, F. Mavré, D. Lorcy, M. Fourmigué and B. Schöllhorn, *Phys. Chem. Chem. Phys.*, 2016, **18**, 15867–15873.